Molecular Therapy
Oncology
Brief report

Engineering a novel HSV-1 strain for oncolytic therapy of solid tumors

Karina Vázquez-Arreguín,[1] Alex Gonzalez,[2] Amy Webb,[3] Xiaokui Mo,[3] Yoshihiro Otani,[4] and Balveen Kaur[1]

[1]Department of Pathology, Georgia Cancer Center at Augusta University, Augusta, GA 30912, USA; [2]Department of Neurosurgery, UTHealth Houston, Houston, TX 77030, USA; [3]Department of Biomedical Informatics, The Ohio State University, Columbus, OH 43210, USA; [4]Department of Neurological Surgery, Okayama University Graduate School of Medicine, Dentistry, and Pharmaceutical Sciences, Okayama 700-8558, Japan

Oncolytic herpes simplex virus (HSV)-1-derived viruses are being developed for cancer treatment. Here, we describe the isolation of a novel strain of HSV-1 and its engineering to safely harness it as an oncolytic therapeutic. This strain (UT1a) was isolated from a de-identified consented patient biorepository. CRISPR-Cas9-based recombination was utilized to insert bacterial artificial chromosome (BAC) genes into the viral *UL39* and *UL40* locus, resulting in the deletion of both large and small subunits of the viral ribonucleotide reductase (RR). Subsequent deletion of viral *RL1* genes encoding the neurovirulence factor γ34.5 resulted in OncoDelta (OncoD), a virus deleted for *UL39*, *UL40*, and both copies of *RL1*. OncoD retained tumor-cell-specific cytotoxicity and replication; was safe and non-toxic in intracranial injections in naive mice up to doses of 5×10^6, the maximal injectable dose for OncoD; and showed significant anti-tumor immune-activating potential in multiple tumor models. Transcriptome profiling of OncoD showed that it impaired DNA damage repair pathways and hence synergized with radiation to improve therapeutic response *in vitro* and *in vivo*.

INTRODUCTION

Oncolytic viruses are an emerging biotherapy, and they function through the direct destruction of tumor cells, releasing tumor antigens to prime anti-tumor immunity.[1,2] While there are currently many viruses that are being investigated, two herpes simplex virus (HSV)-1-based virotherapies have garnered approval for treatment so far. Imlygic is approved in the USA and Europe for the treatment of advanced melanoma, and DELYTACT is approved in Japan for the treatment of recurrent glioblastoma (GBM).[3,4] The Imlygic virus currently approved in the USA and European Union (EU) for melanoma is deleted for both copies of the *RL1* gene (encoding for ICP34.5) and harbors an additional deletion in the ICP47 gene. This virus retains *UL39* and *UL40* genes. Imlygic is additionally armed with granulocyte-macrophage colony-stimulating factor (GM-CSF) to increase anti-tumor immune responses. DELYTACT is an unarmed, triple-mutated oncolytic virus that is disrupted for *UL39* and deleted for both copies of ICP34.5 and also harbors a deletion in the ICP47 gene. The potential to employ these viruses as additional gene therapy vehicles to further improve tumor cell killing and augment anti-tumor immune responses is an important avenue of research,[5–7] and having a viral backbone that permits the insertion of therapeutic payloads with ease is important. Recombination-driven gateway-designed viruses have facilitated efficient viral loading with genetic payloads.[8,9] Here, we isolated a new strain of HSV-1, UT1a, from a de-identified consented patient biorepository to engineer an oncolytic HSV (oHSV). UT1a was significantly better at killing tumor cells compared to F-strain HSV-1. Deletion of viral neurovirulence genes resulted in the generation of OncoDelta (OncoD), a triple-gene-deleted oHSV-1 virus that remains safe in non-tumor-bearing mice, is sensitive to antiherpetic agents, and has demonstrated therapeutic efficacy in multiple tumor models. The OncoD viral backbone described here is deleted for both copies of ICP34.5 as well as for *UL39* and *UL40* but retains the wild-type (WT) ICP47 gene.

RESULTS

The UT1a strain of HSV-1 was derived from a human labial lesion from a consented patient under an approved institutional review board (IRB) protocol at the University of Texas, Health Sciences Center at Houston. After isolation, the isolated strain was propagated in Vero cells (Figure 1A). The cytotoxicities of WT HSV-1 strains UT1a and F-strain were compared in a panel of tumor cells (Figure 1B). UT1a was observed to be more cytotoxic toward tumor cells compared to F-strain. To facilitate genomic manipulations of the viral genome, we utilized CRISPR-Cas9-guided homologous recombination (HR) to insert flippase recognition target (FRT) sites and *loxP*-flanked bacterial artificial chromosome (BAC) genes into the *UL39*/*UL40* locus (Figure 1C).[8] DNA sequencing of the BAC genome confirmed the insertion of the BAC sequences and the loss of *UL39*/*UL40* (Figure S1A). Next, the γ34.5-expressing genes (*RL1*) were targeted by HR in bacteria, and the loss of *RL1* was confirmed by PCR (Figure S1B).

The GFP-containing BAC sequence inserted into the *UL39*/*UL40* locus was designed to be flanked by FRT (blue arrow) and *loxP* (red arrow) recombination sites (Figure 1C). To easily insert transgenes (e.g.,

Received 21 October 2024; accepted 24 February 2025;
https://doi.org/10.1016/j.omton.2025.200961.

Correspondence: Balveen Kaur, Department of Pathology, Georgia Cancer Center at Augusta University, Augusta, GA 30912, USA.
E-mail: bkaur@augusta.edu

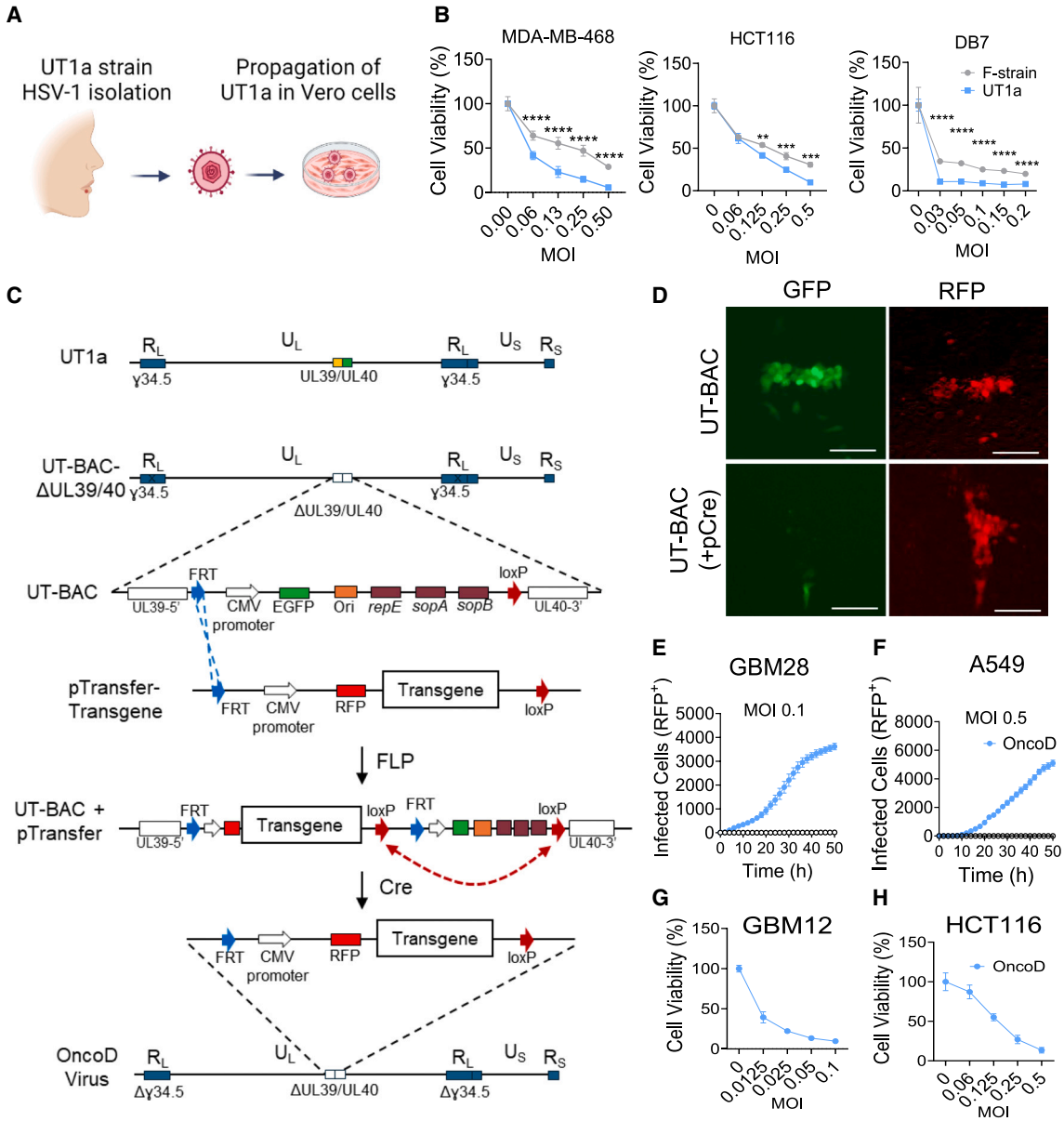

Figure 1. Generation of triple-mutated oncolytic HSV-1 OncoD from UT1a strain

(A) HSV-1 strain UT1a was isolated from a consented patient's labial lesion and propagated in Vero cells. (B) Human tumor cells MDA-MB-468 and HCT116 and mouse DB7 cells were infected with UT1a and F-strain HSV-1 at the indicated MOIs for 72 h. (C) Schematic of mutations in UT1a to generate OncoD. (D) Immunofluorescence imaging of Vero cells transfected with UT-BAC with and without Cre-mediated recombination to remove the bacterial sequences, including GFP. Scale bar, 100 μm. (E and F) Analysis of OncoD replication in human cell lines GBM28 (E) and A549 (F) at the indicated MOIs. (G and H) Cytotoxicity analysis of OncoD against human tumor cells GBM12 (G) and HCT116 (H). $^{**}p < 0.01$, $^{***}p < 0.001$, and $^{****}p < 0.0001$.

RFP) into the oncolytic virus backbone, FRT-based recombination between the BAC and an FRT-containing transfer plasmid encoding for the RFP and containing a *loxP* site was used. This recombination inserted the entire RFP-containing transfer plasmid into the BAC (blue dotted line, Figure 1C) to generate UT-BAC + pTransfer. A subsequent recombination between the *loxP* sites (red dotted lines) enables the removal of the bacterial transfer plasmid and BAC bacterial sequences from the UT-BAC + pTransfer backbone. Thus, before Cre-lox recombination, the transfected cells are both RFP^+ and GFP^+, but once the bacterial sequences are excised out, the resulting virus loses GFP and retains the inserted transgene (RFP) (Figure 1D). The loss of ICP34.5 was validated by genomic PCR of the virus (Figure S1B) and by western blot for phosphorylated eIF2α (p-eIF2α) (Figure S1C). ICP34.5 in the WT virus dephosphorylates eIF2α,

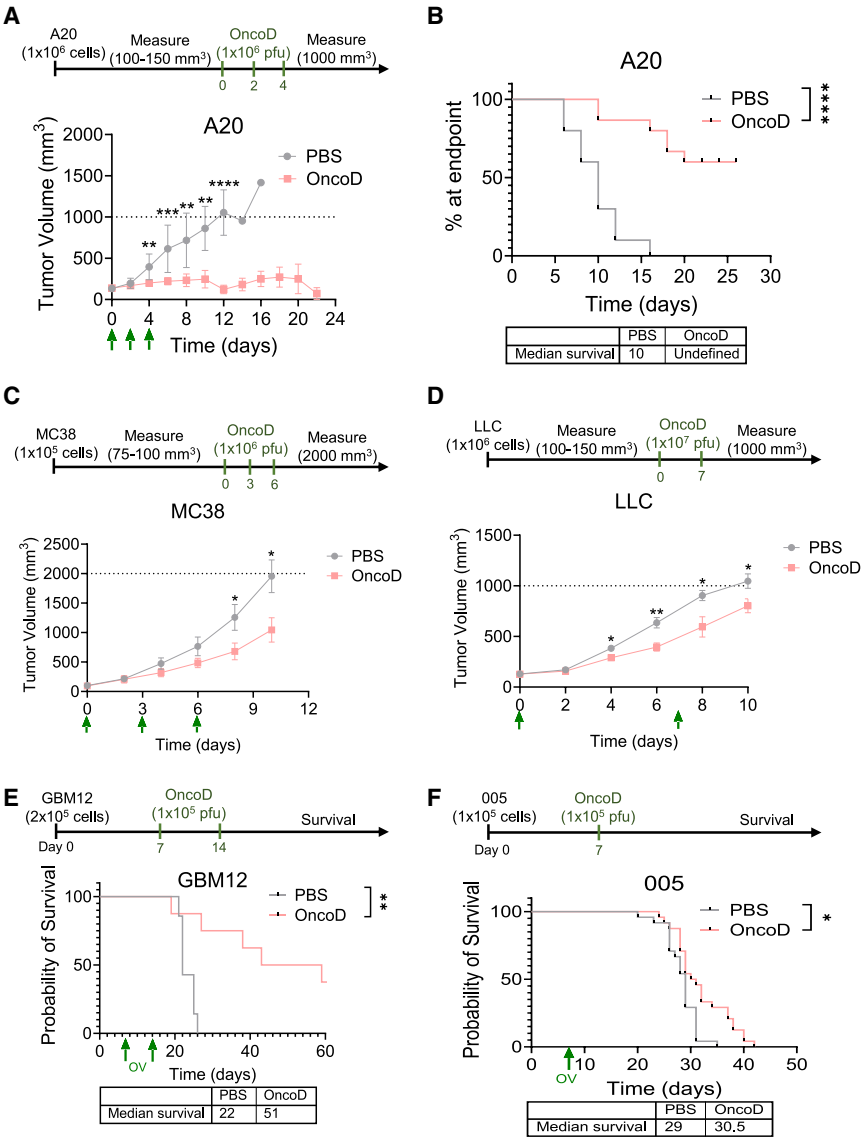

Figure 2. OncoD is safe at high doses in mice and improves survival in multiple *in vivo* mouse tumor models

(A) Effect of OncoD on syngeneic A20 subcutaneous tumor growth in BALB/c mice. Once tumors reached the indicated tumor volume, OncoD or PBS was injected intratumorally at the indicated time points (green arrows). After treatment, tumor volumes were measured every other day. (B) Kaplan-Meier curve showing the proportion of mice reaching the established endpoint tumor volume over time. (C and D) Effect of OncoD on syngeneic MC38 (C) and LLC (D) subcutaneous tumor growth in C57BL6 mice. (E) Kaplan-Meier curve showing the effect of OncoD on the survival of NSG mice bearing intracranial human GBM12 tumors. OncoD was administered intratumorally at the indicated time points (green arrows). (F) Kaplan-Meier curve showing the effect of OncoD on the survival of C57BL6 mice bearing 005 mouse glioma tumors. $^{*}p < 0.05$, $^{**}p < 0.01$, $^{***}p < 0.001$, and $^{****}p < 0.0001$.

and thus treatment with WT HSV-1 (F-strain and UT1a) shows reduced p-eIF2α. ICP34.5-deleted viruses are unable to reverse protein kinase RNA-activated (PKR)-induced eIF2α phosphorylation, so these viruses show increased phosphorylation of eIF2α.

Real-time imaging of RFP^{+}-infected cells revealed efficient OncoD replication in tumor cells (Figures 1E and 1F) but not in normal cells (Figures S2A and S2B). We then compared the replication of OncoD (*ΔRL1*, *ΔUL39*, and *ΔUL40*) virus to a previously published oncolytic HSV (oHSVQ) virus that is a double-deleted virus (*ΔRL1* and *ΔUL39*), similar to G207 in the clinical investigation[8]. Real-time fluorescent imaging of infected cells over time revealed that while the kinetics of OncoD and HSVQ were similar (same slopes of virus spread over time), the viral replication (burst size) was higher for OncoD. This permitted a higher yield of OncoD from Vero cell production runs (Figures S2C and S2D). We next evaluated the cytotoxicity of OncoD and saw efficient killing of tumor cells with increasing multiplicity of infection (MOI) (Figures 1G, 1H, S2E, and S2F). Notably, despite the triple deletion and consistent with a similar kinetics of virus spread *in vitro*, the cytotoxicity of OncoD was similar to oHSVQ in treated tumor cells (Figures S2G and S2H). No cytotoxicity was observed in the normal cells tested with OncoD (Figures S2I and S2J) or with both OncoD and oHSVQ (Figure S2K) at MOIs as high as 1, and thus no LD50 could be calculated from these cells (Figure S2L).

To determine if OncoD retained sensitivity to acyclovir (ACV), an antiherpetic agent,[10] we evaluated its cytotoxicity toward Vero cells in the presence and absence of ACV. ACV conferred 95.3% ± 6.3% protection from OncoD-mediated cytotoxicity (Figure S3A), which was similar to that observed with oHSVQ (Figure S3B). Due to the increased viral replication of OncoD compared to oHSVQ, viral titers from each virus purification were significantly higher, allowing for the evaluation of higher doses *in vivo* (Figure S3C). To evaluate the clinical utility of OncoD, we evaluated its safety profile in mice. Intracerebral inoculation of 5×10^2 plaque-forming units (PFUs) of UT1a virus in non-tumor-bearing adult mice was toxic in 4/5 mice. However, injections of OncoD up to doses as high as 5×10^6 PFUs (maximum injectable dose) were found to be safe and well tolerated in naive mice (Figure S3D). In comparison, the maximum injectable dose for oHSVQ was 1×10^6 PFUs, at which it remained safe. The different tested doses and the response in mice are listed in Figure S3E.

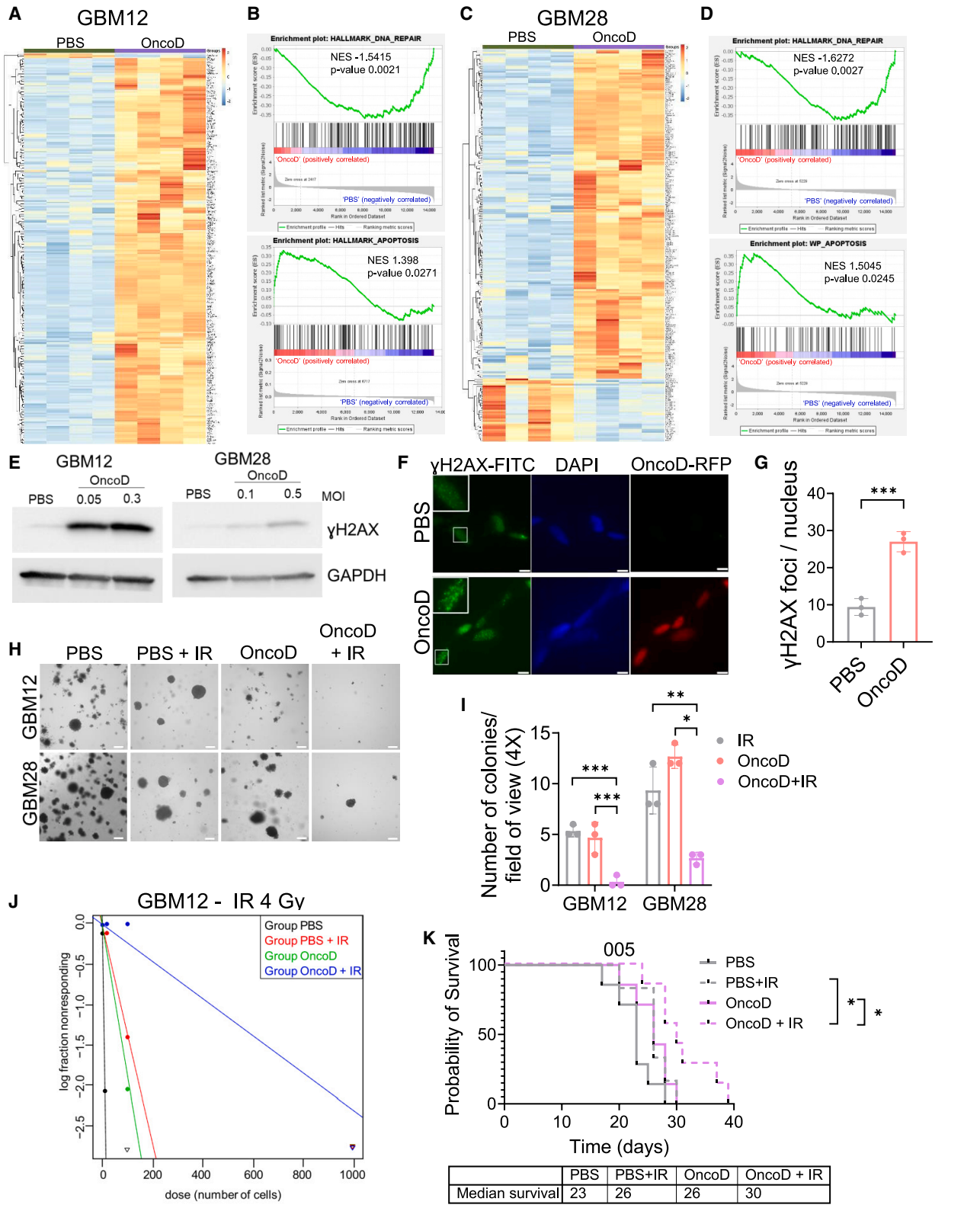

	PBS	PBS+IR	OncoD	OncoD + IR
Median survival	23	26	26	30

(legend on next page)

We next evaluated the *in vivo* efficacy of OncoD in mouse tumor models. Treatment with OncoD was found to be effective against human tumors in NSG (*NOD.Cg-Prkdc*^{scid}*IL2rg*^{tm1Wjl}/SzJ) mice (GBM12) and syngeneic murine tumors in immunocompetent mice (A20, LLC, and MC38) (Figures 2A–2F). Transcriptomic analysis of human glioma cells (GBM12 and GBM28) treated with or without OncoD revealed a significant enrichment of pathways related to apoptosis and DNA repair relative to untreated cells (Figures 3A–3D). Significantly de-regulated genes in OncoD-infected GBM cells relative to PBS control are listed in Tables S1 and S2. To check for increase in DNA damage in cells treated with OncoD, we analyzed the levels of γH2AX phosphorylation by western blot and immunofluorescence. Infection with OncoD induced γH2AX protein levels (Figures 3E–3G). DNA repair plays a significant role in response to chemo- and radiation therapy, and this suggested that OncoD might synergize with radiation therapy (IR) to improve outcomes. To evaluate this, we measured the clonogenic capacity of OncoD-treated cells with and without radiation. Both spheroid formation and limited dilution assays showed a significant reduction in the clonogenic capacity of cells treated with both OncoD and irradiation (Figures 3H–3J). In immunocompetent mice, the combined treatment of OncoD and radiation (2 Gy) significantly improved survival compared to either monotherapy (Figure 3K).

DISCUSSION

Here, we describe the engineering of a triple-gene-deleted HSV-1-derived oncolytic virus. The attenuations in the expression of *UL39*, *UL40*, and *RL1* gene products imparted tumor specificity. *UL39* and *UL40* encode for the large and small subunits of ribonucleotide reductase (RR) and are, hence, essential to initiate nucleotide metabolism in quiescent cells. In mammalian cells, this is regulated by the Rb pathway, and its loss in tumor cells provides unrestricted access to the cellular RR, which compensates for this attenuation.[11,12] Deletion of the *UL39/UL40* locus was verified by genomic sequencing. To our knowledge, this is the only oncolytic virus that has been attenuated for both RR subunits. The viral *RL1* gene encodes for a multifunctional ICP34.5 that helps HSV-1 counter numerous anti-viral defense responses and also plays a role in latent HSV-1 reactivation.[13,14] Cellular EIF2AK2 senses infection and phosphorylates cellular eIF2α to block protein translation and, hence, virus replication. Viral ICP34.5 reverses EIF2AK2 phosphorylation by PKR to facilitate viral replication.[15,16] The lack of functional ICP34.5 in OncoD was validated by PCR and western blot analysis. Interestingly, despite the three mutations in OncoD (UT1a strain), compared to only two deletions in HSVQ (F-strain), OncoD has a bigger viral burst than HSVQ and consistently gave a better viral yield.

Apart from having a better viral yield and exhibiting tumor-cell-specific cytotoxicity, OncoD also remains sensitive to ACV and is safe upon intracerebral injections in mice. The treatment of tumor-bearing mice with OncoD showed increased therapeutic benefit with and without radiation. Given the safe and effective profile of OncoD in multiple different tumor models, its further development as an anti-neoplastic agent is recommended.

MATERIALS AND METHODS

Additional methods are detailed in the supplemental information.

Animal studies

All animal studies were conducted with the approval of the Augusta University Institutional Animal Care and Use Committee. NSG (stock #005557), C57BL/6 (stock #000664) and BALB/c (stock #000651) were obtained from Jackson Laboratory. Intracranial injections were performed as described.[5] For the establishment of subcutaneous tumor models, 1×10^5 MC38 cells were injected into the right flank in 100 μL of PBS. The formation of tumors was monitored daily, and once tumors reached 70–100 mm^3, the mice were divided randomly into PBS or OncoD treatment groups. OncoD (1×10^7 PFUs) or PBS was administered at days 0, 3, and 6, and tumor volumes were measured every other day until endpoint (2,000 mm^3). For LLC and A20 models, 1×10^6 cells were injected into the right flank in 100 μL of PBS in C57BL6 and BALB/c mice, respectively. Once tumors reached 100–150 mm^3, mice were randomly divided into treatment groups. OncoD was administered at 1×10^7 PFUs in LLC tumors on days 0 and 7 and at 1×10^6 PFUs on days 0, 2, and 4 in A20 tumors. Tumors were measured every other day, and when the tumor volume reached 1,000 mm^3, the mice were sacrificed.

DATA AND CODE AVAILABILITY

Processed and raw RNA-seq data are available at the Gene Expression Omnibus Database (accession no. GEO: GSE288846). Source data from this manuscript are available from the corresponding author upon reasonable request.

ACKNOWLEDGMENTS

We wish to acknowledge the valuable help of the expert personnel at the Integrated Genomics Shared Resources Georgia Cancer Center (M. Zoccheddu, M. Yu, and S.S. Manam) and the Center for Biotechnology & Genomic Medicine (N. Sinha and A. Sharma). The project described was supported by an Underrepresented Population Fellowship Award in Gene and Cell Therapy to K.V.-A. The content is solely the responsibility of the authors and does not necessarily represent the official views of the American Society of Gene & Cell Therapy. B.K. was supported by grants NIH/ NCI P01CA163205 and NIH/ NINDS R61NS112410, R61NS128191, and R01NS127473.

AUTHOR CONTRIBUTIONS

K.V.-A. designed and performed experiments, analyzed data, and wrote the manuscript. A.G. assisted with the genomic modifications of UT-BAC. A.W. and X.M. performed the genomic sequencing and alignments of the UT-BAC to the UT1a and F-strain genomes.

Figure 3. OncoD induces DNA damage in infected tumor cells and synergizes with radiation

(A–D) Heatmaps and significantly enriched gene set enrichment analysis (GSEA) pathways altered upon treatment with OncoD in the indicated cells. (E–G) Western blot (GBM12 and GBM28 cells, E) and immunofluorescence analysis (GBM12 cells, F) for γH2AX phosphorylation after treatment with OncoD and quantification of γH2AX foci (G). Scale bar, 10 μm. (H–J) Reduced colony formation in the indicated glioma cells after treatment with radiation (4 Gy) and OncoD. Scale bar, 200 μm. (K) Kaplan-Meier survival curve showing the effect of OncoD combination with IR in the mouse glioma 005 model. $^*p < 0.05$, $^{**}p < 0.01$, and $^{***}p < 0.001$.

Y.O. assisted with the characterization of UT1a and cytotoxicity comparison between UT1a and F-strain. B.K. conceived the idea, supervised the project, and assisted with the writing of the manuscript. All authors read, edited, and approved the manuscript.

DECLARATION OF INTERESTS

The authors declare no competing interests.

SUPPLEMENTAL INFORMATION

Supplemental information can be found online at https://doi.org/10.1016/j.omton.2025.200961.

REFERENCES

1. Epstein, A.L., and Rabkin, S.D. (2024). Safety of non-replicative and oncolytic replication-selective HSV vectors. Trends Mol. Med. *30*, 781–794. https://doi.org/10.1016/j.molmed.2024.05.014.
2. Ling, A.L., Solomon, I.H., Landivar, A.M., Nakashima, H., Woods, J.K., Santos, A., Masud, N., Fell, G., Mo, X., Yilmaz, A.S., et al. (2023). Clinical trial links oncolytic immunoactivation to survival in glioblastoma. Nature *623*, 157–166. https://doi.org/10.1038/s41586-023-06623-2.
3. Todo, T., Ito, H., Ino, Y., Ohtsu, H., Ota, Y., Shibahara, J., and Tanaka, M. (2022). Intratumoral oncolytic herpes virus G47Δ for residual or recurrent glioblastoma: a phase 2 trial. Nat. Med. *28*, 1630–1639. https://doi.org/10.1038/s41591-022-01897-x.
4. Larocca, C.A., LeBoeuf, N.R., Silk, A.W., and Kaufman, H.L. (2020). An Update on the Role of Talimogene Laherparepvec (T-VEC) in the Treatment of Melanoma: Best Practices and Future Directions. Am. J. Clin. Dermatol. *21*, 821–832. https://doi.org/10.1007/s40257-020-00554-8.
5. Russell, L., Swanner, J., Jaime-Ramirez, A.C., Wang, Y., Sprague, A., Banasavadi-Siddegowda, Y., Yoo, J.Y., Sizemore, G.M., Kladney, R., Zhang, J., et al. (2018). PTEN expression by an oncolytic herpesvirus directs T-cell mediated tumor clearance. Nat. Commun. *9*, 5006. https://doi.org/10.1038/s41467-018-07344-1.
6. Ring, E.K., Li, R., Moore, B.P., Nan, L., Kelly, V.M., Han, X., Beierle, E.A., Markert, J.M., Leavenworth, J.W., Gillespie, G.Y., and Friedman, G.K. (2017). Newly Characterized Murine Undifferentiated Sarcoma Models Sensitive to Virotherapy with Oncolytic HSV-1 M002. Mol. Ther. Oncolytics *7*, 27–36. https://doi.org/10.1016/j.omto.2017.09.003.
7. Thomas, S., Kuncheria, L., Roulstone, V., Kyula, J.N., Mansfield, D., Bommareddy, P.K., Smith, H., Kaufman, H.L., Harrington, K.J., and Coffin, R.S. (2019). Development of a new fusion-enhanced oncolytic immunotherapy platform based on herpes simplex virus type 1. J. Immunother. Cancer *7*, 214. https://doi.org/10.1186/s40425-019-0682-1.
8. Terada, K., Wakimoto, H., Tyminski, E., Chiocca, E.A., and Saeki, Y. (2006). Development of a rapid method to generate multiple oncolytic HSV vectors and their *in vivo* evaluation using syngeneic mouse tumor models. Gene Ther. *13*, 705–714. https://doi.org/10.1038/sj.gt.3302717.
9. Hu, J.C., Booth, M.J., Tripuraneni, G., Davies, D., Zaidi, S.A.A., Tamburo de Bella, M., Slade, M.J., Marley, S.B., Gordon, M.Y.A., Coffin, R.S., et al. (2006). A novel HSV-1 virus, JS1/34.5-/47-purges contaminating breast cancer cells from bone marrow. Clin. Cancer Res. *12*, 6853–6862. https://doi.org/10.1158/1078-0432.CCR-06-1228.
10. Field, H.J., and Vere Hodge, R.A. (2013). Recent developments in anti-herpesvirus drugs. Br. Med. Bull. *106*, 213–249. https://doi.org/10.1093/bmb/ldt011.
11. Aghi, M., Visted, T., Depinho, R.A., and Chiocca, E.A. (2008). Oncolytic herpes virus with defective ICP6 specifically replicates in quiescent cells with homozygous genetic mutations in p16. Oncogene *27*, 4249–4254. https://doi.org/10.1038/onc.2008.53.
12. Mineta, T., Rabkin, S.D., and Martuza, R.L. (1994). Treatment of malignant gliomas using ganciclovir-hypersensitive, ribonucleotide reductase-deficient herpes simplex viral mutant. Cancer Res. *54*, 3963–3966.
13. Manivanh, R., Mehrbach, J., Knipe, D.M., and Leib, D.A. (2017). Role of Herpes Simplex Virus 1 gamma34.5 in the Regulation of IRF3 Signaling. J. Virol. *91*, e01156-17. https://doi.org/10.1128/JVI.01156-17.
14. Mattila, R.K., Harila, K., Kangas, S.M., Paavilainen, H., Heape, A.M., Mohr, I.J., and Hukkanen, V. (2015). An investigation of herpes simplex virus type 1 latency in a novel mouse dorsal root ganglion model suggests a role for ICP34.5 in reactivation. J. Gen. Virol. *96*, 2304–2313. https://doi.org/10.1099/vir.0.000138.
15. Manivanh, R., Mehrbach, J., Charron, A.J., Grassetti, A., Cerón, S., Taylor, S.A., Cabrera, J.R., Gerber, S., and Leib, D.A. (2020). Herpes Simplex Virus 1 ICP34.5 Alters Mitochondrial Dynamics in Neurons. J. Virol. *94*, e01784-19. https://doi.org/10.1128/JVI.01784-19.
16. Davis, K.L., Korom, M., and Morrison, L.A. (2014). Herpes simplex virus 2 ICP34.5 confers neurovirulence by regulating the type I interferon response. Virology *468–470*, 330–339. https://doi.org/10.1016/j.virol.2014.08.015.